Biochimica et Biophysica Acta 1798 (2010) 688–699

Contents lists available at ScienceDirect

Biochimica et Biophysica Acta

journal homepage: www.elsevier.com/locate/bbamem

Liquid-ordered phases induced by cholesterol: A compendium of binary phase diagrams

Derek Marsh

Max-Planck-Institut für biophysikalische Chemie, Abteilung Spektroskopie und photochemische Kinetik, 37070 Göttingen, Germany

ARTICLE INFO

Article history:
Received 16 October 2009
Received in revised form 8 December 2009
Accepted 29 December 2009
Available online 7 January 2010

Keywords:
Membrane domain
Lateral phase separation
Lipid phase diagram
Cholesterol
Lipid raft

ABSTRACT

Mixtures of phospholipids with cholesterol are able to form liquid-ordered phases that are characterised by short-range orientational order and long-range translational disorder. These L_o-phases are distinct from the liquid-disordered, fluid L_α-phases and the solid-ordered, gel L_β-phases that are assumed by the phospholipids alone. The liquid-ordered phase can produce spatially separated in-plane fluid domains, which, in the form of lipid rafts, are thought to act as platforms for signalling and membrane sorting in cells. The areas of domain formation are defined by the regions of phase coexistence in the phase diagrams for the binary mixtures of lipid with cholesterol. In this paper, the available binary phase diagrams of lipid–cholesterol mixtures are all collected together. It is found that there is not complete agreement between different determinations of the phase diagrams for the same binary mixture. This can be attributed to the indirect methods largely used to establish the phase boundaries. Intercomparison of the various data sets allows critical assessment of which phase boundaries are rigorously established from direct evidence for phase coexistence.

1. Introduction

The liquid-ordered phase (L_o), a lamellar lipid assembly with short-range orientational order but long-range translational disorder [1], has assumed a central position in the discussion of lipid rafts that are proposed as functional platforms in cellular signalling and intracellular membrane traffic [2,3].

In binary lipid mixtures with cholesterol, the L_o-phase is experimentally established as a bona-fide phase in coexistence with the solid-ordered $L_{\beta(')}$ gel phase at temperatures below the chain-melting temperature, T_m, of the phospholipid component. The principal evidence for this comes from two-component quadrupolar ^{2}H-NMR spectra of lipids with deuterated chains [4,5], but also correspondingly from broad-line ^{13}C-NMR spectra of *sn*-2 carbonyl-labelled lipids [6].

Direct evidence for fluid–fluid coexistence of L_o and liquid-disordered (L_α) phases – the situation that is most likely to parallel domain formation in natural membranes – is, however, relatively rare. In particular, fluorescence microscopy, which has proved so successful in visualising coexistence of macroscopic fluid domains in giant unilamellar vesicles (GUVs) composed of ternary mixtures that include cholesterol, has been unable to detect formation of domains in binary mixtures of cholesterol with a single lipid ([7–9], and see also [10]). However, this non-observation of domain coexistence extends also to the gel phase of the binary mixtures [11] and also to the fluid regime of certain ternary lipid mixtures [12]. Similarly, coexisting fluid domains were visualised recently for ternary lipid mixtures with cholesterol from high-angle X-ray diffraction of oriented membranes [13], but not for binary mixtures with cholesterol [13,14].

With a biradical spin-labelled lipid, coexisting fluid domains were visualised directly as two-component EPR spectra in mixtures of dipalmitoylphosphatidylcholine, $(16:0)_2$PC, with cholesterol [15]. Two-component spectra of spin-labelled lipids have been found in fluid-phase mixtures of *N*-palmitoylsphingomyelin [SM(d18:1/16:0)] with cholesterol [16]. Recently, two-component ^{2}H-NMR spectra of deuterated dipalmitoylphosphatidylcholine [d_{62}-$(16:0)_2$PC] in mixtures with cholesterol were also resolved at temperatures above the chain-melting temperature of the perdeuterated lipid [17]. In contrast to these isolated examples in which L_α–L_o phase coexistence is demonstrated directly, a large number of phase diagrams have been proposed for cholesterol-containing binary mixtures, in which the phase boundaries of L_α–L_o phase coexistence are determined indirectly.

Here, I collect together the published binary phase diagrams for mixtures of various lipids with cholesterol, in order to compare and contrast those obtained by the different indirect experimental methods. By doing this, it is possible to examine critically the true extent of the evidence for L_α–L_o phase coexistence in mixtures of a single lipid with cholesterol. This should help to establish whether a minimal requirement for raft formation is the combination of a low-melting lipid with a high-melting lipid and cholesterol, such as in the "canonical" model lipid raft mixture of 1-palmitoyl-2-oleoyl phosphatidylcholine [(16:0/18:1cΔ^9)PC] with SM(d18:1/16:0) and cholesterol.

E-mail address: dmarsh@gwdg.de.

0005-2736/$ – see front matter © 2010 Elsevier B.V. All rights reserved.
doi:10.1016/j.bbamem.2009.12.027

It should be noted that, although data points are taken from the original publications, phase boundaries and phase assignments are given by me, in light of the present state of the field, and may not necessarily correspond exactly with those originally published.

2. Binary phase diagrams and three-phase lines

A crucial feature in the discussion of binary phase diagrams is the occurrence of three-phase lines at temperatures close to those of chain-melting (i.e., T_m) for the single lipid species. For a two-component lipid mixture ($C=2$) in excess water at constant pressure, the Gibbs phase rule states that the number of degrees of freedom, F, of the system is given by (see, e.g., [18]):

$$F = C\text{–}P + 1 \tag{1}$$

where P is the number of coexisting phases. Thus when three phases coexist ($P=3$), the number of degrees of freedom is $F=0$. Gel (L_β), liquid-ordered (L_o) and liquid-disordered (L_α) phases may therefore only coexist at constant temperature, i.e., along a horizontal phase boundary, where the compositions of all phases are constant (determined by the ends of the tie line) — see Fig. 1. Below the three-phase line, L_β and L_o phases coexist, and above the three-phase line, L_α and L_o phases coexist. Thus the occurrence of a horizontal upper phase boundary for the region of L_β–L_o coexistence automatically implies the coexistence of L_α and L_o phases at temperatures immediately above this phase boundary. This latter result is a thermodynamic inevitability for large systems. As regards this implied L_α–L_o fluid phase coexistence in binary mixtures, the critical question experimentally is, therefore, to what extent the upper phase boundary of the L_β–L_o coexistence region is truly horizontal. An associated question is the extent to which the approximation of large systems holds (see the discussion in [19]). If domains are small, the interfaces between domains may constitute a significant part of the system and introduce one more degree of freedom [20], which would make the requirement for a horizontal line no longer exact.

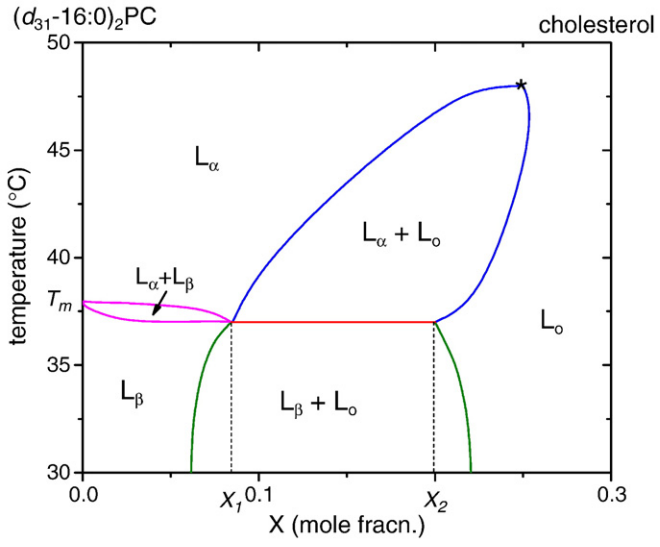

Fig. 1. Generic phase diagram for binary mixtures of a single lipid with cholesterol dispersed in excess water. Phase boundaries are those for chain-perdeuterated dipalmitoylphosphatidylcholine, $(d_{31}$-16:0$)_2$PC [4,17]. L_β, gel phase; L_α, fluid (disordered) phase; L_o, liquid-ordered phase. Single-phase regions (L_α, L_β, L_o) and two-phase regions ($L_\beta+L_\alpha$, $L_\beta+L_o$, $L_\alpha+L_o$) are indicated. Asterisk indicates the approximate position of a critical point. The red horizontal line at constant temperature indicates coexistence of L_α or L_β phases containing mole fraction X_1 of cholesterol together with L_o phase containing mole fraction X_2 of cholesterol.

In the two-phase regions, above and below the three-phase line for extended systems, the fractions, f_{Lo}, of L_o phase at fixed temperature are given by the lever rule [18]. For L_α–L_o fluid phase coexistence, for example, the dependence on mole fraction, X, of cholesterol is given by:

$$f_{Lo} = \frac{X - X_{L\alpha}}{X_{Lo} - X_{L\alpha}} \tag{2}$$

where X_{Lo} and $X_{L\alpha}$ are the mole fractions of cholesterol in the coexisting L_o and L_α phases along a tie line at constant temperature. The fractional population of L_o phase therefore depends linearly on the mole fraction of cholesterol. For the L_α phase, the corresponding fractional population is simply given by: $f_{L\alpha} = 1 - f_{Lo}$. The fraction, f, of a spectroscopic probe (fluorescent or spin label) in the L_o phase depends additionally on the partition coefficient, K_p, between the L_o and L_α phases [21,22]:

$$f = \frac{K_p(X - X_{L\alpha})}{X_{Lo} - X_{L\alpha} + (K_p - 1)(X - X_{L\alpha})} \tag{3}$$

where again the fraction of probe in the L_α phase is $1-f$. Therefore, only for equipartitioning between the two phases, i.e., $K_p = 1$, does the fractional population of probe depend linearly on the mole fraction of cholesterol (compare Eqs. (2) and (3)).

3. Phosphatidylcholine–cholesterol mixtures

3.1. Dipalmitoylphosphatidylcholine (16:0)$_2$PC/cholesterol

Fig. 2A–F shows the various different phase diagrams that have been proposed for hydrated binary mixtures of (16:0)$_2$PC with cholesterol. Fig. 2A gives the phase diagram that first directly demonstrated the L_o-phase as a separate phase in coexistence with L_β gel-phase lipid, from the two-component ^{2}H-NMR powder spectra obtained at temperatures below T_m [4]. (Note that the phase boundaries for this particular system are shown enlarged in Fig. 1.) The lipid chains are perdeuterated, (d_{31}-16:0)$_2$PC, which results in a lower chain-melting temperature of the PC alone than that for its completely protiated counterpart. The horizontal three-phase line is established mostly from calorimetry. Direct evidence was not found for L_α–L_o fluid-phase coexistence, except that as already mentioned, two-component spectra have now been identified at temperatures above that of chain-melting of the lipid (see triangles in Fig. 2A [17]). These points lie close to, although slightly outside, the L_α–L_o coexistence region in Fig. 2A, but would be accommodated within the corresponding region for other phase diagrams in Fig. 2 (viz., Fig. 2B, C, E and F). The upper boundaries shown for L_α–L_o phase separation in Fig. 2A are not established directly, but instead are inferred from line broadening/narrowing of the single-component fluid-phase ^{2}H-NMR spectra and broadening towards high temperatures of the (reduced) calorimetric peak in excess heat capacity. The positions of these boundaries have been revised recently [17] from those of the original publication [4]. The region of L_α–L_o coexistence forms a closed loop which suggests the existence of a critical point at which the L_α and L_o phases become indistinguishable (see Fig. 1). Such a situation is accompanied by large compositional fluctuations that could be manifest as extreme broadening of NMR lines (see refs. [17,23]). Note that, for a spectroscopy with shorter timescale, these compositional fluctuations may cause appearance of two-component spectra without being in a region of phase coexistence (see, e.g., [24]).

Fig. 2B shows the phase diagram proposed for the fluid coexistence region by using measurements of hyperfine anisotropy from a spin-labelled phosphatidylcholine probe. Two-component EPR spectra, such as result from coexisting phases [10,16], were not observed.

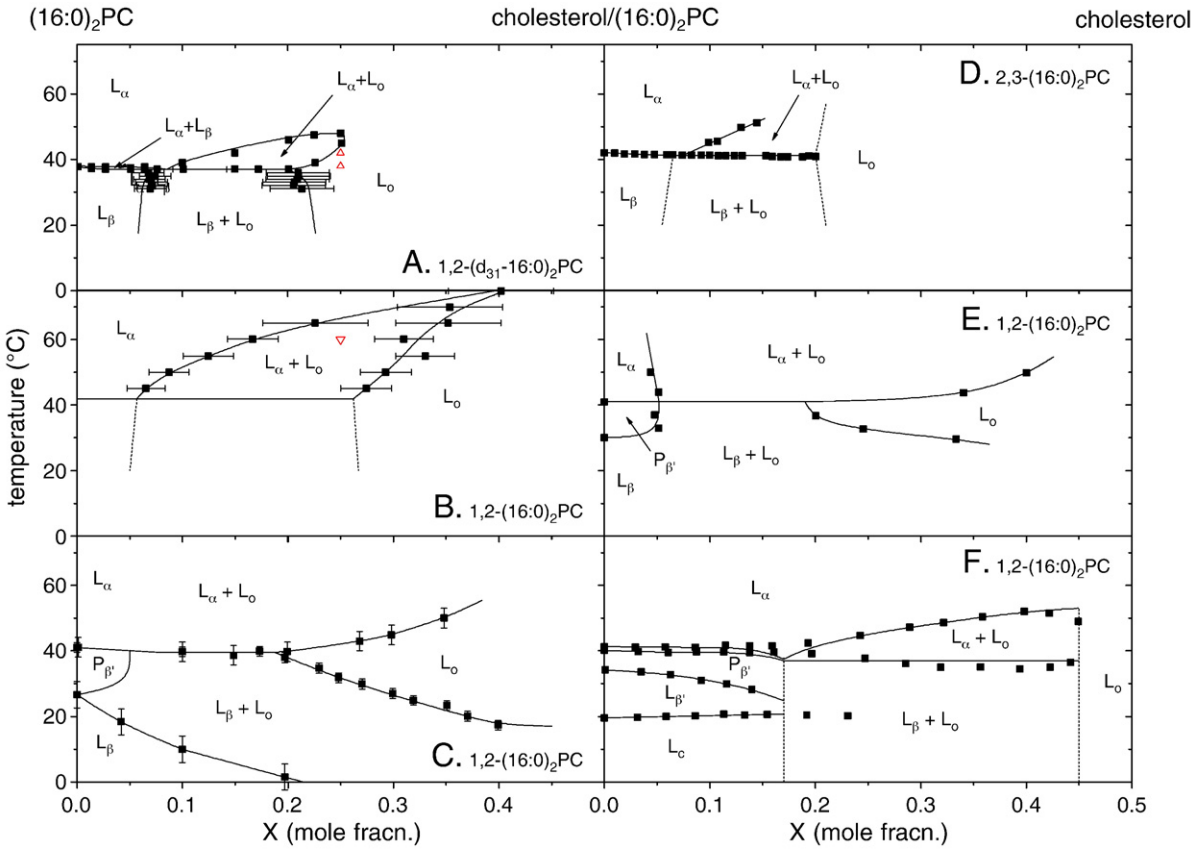

Fig. 2. Binary phase diagrams for mixtures of dipalmitoylphosphatidylcholine, $(16:0)_2$PC, with cholesterol in excess water. A. 1,2-(d_{31}-16:0)$_2$PC with perdeuterated chains. Data from ref. [4] with revised data for the fluid regime from ref. [17]. Based mostly on ^{2}H-NMR with some calorimetry (DSC). Triangles represent points for which L_α–L_o phase coexistence is detected from two-component ^{2}H-NMR spectra [17]. B. Normal protiated 1,2-$(16:0)_2$PC, fluid phases only. Data points from ref. [25]. Based on compositional dependence of outer hyperfine splittings from spin-labelled PC. Inverted triangle represents a point for which the L_α–L_o phase coexistence is detected from two-component EPR spectra of a biradical spin-labelled PC [15]. C. Specifically deuterated or ^{13}C-labelled 1,2-$(16:0)_2$PC. Data points from ref. [26]. Phase boundaries below T_m of 1,2-$(16:0)_2$PC were deduced from ^{13}C-NMR spectra. D. Protiated 2,3-$(16:0)_2$PC isomer. Data points from ref. [28]. Deduced from differential scanning calorimetry (DSC). E. Normal protiated 1,2-$(16:0)_2$PC. Data points from ref. [29]. Deduced from the dependence of acetic acid permeability on composition. F. Normal protiated 1,2-$(16:0)_2$PC. Data points from ref. [30]. L_c is a crystalline lamellar phase. Deduced from DSC measurements. X is the mole fraction of cholesterol.

Instead, phase boundaries were inferred indirectly from discontinuities in slope of the outer hyperfine splitting as a function of cholesterol concentration [25]. This method was also applied by the same workers to infer fluid-phase boundaries for mixtures of $(14:0)_2$PC, $(18:0)_2$PC or brain sphingomyelin with cholesterol that are given later below. In this phase diagram, a critical point is suggested at ca. 74 °C and mole fraction of cholesterol $X \sim 0.4$. Above this temperature, the outer hyperfine splitting changes monotonically with cholesterol content. As already noted, evidence for fluid-phase coexistence was found subsequently in this system by the same workers, from two-component EPR spectra of a biradical spin-labelled phosphatidylcholine (see inverted triangle in Fig. 2B [15]).

Fig. 2C presents a rather different phase diagram for the same system that was deduced from solid-state NMR methods, and calorimetry. Partly phosphatidylcholines with specifically deuterated chains were used, but the main departure in this study was to use lipids with the *sn*-2 carbonyl specifically labelled with ^{13}C [26]. Previous studies had demonstrated that the solid-state ^{13}C-NMR spectra of such lipids can distinguish between gel- and fluid-phase lipids [27], and this was used to investigate the range of L_β–L_o phase coexistence.

At low temperatures, the notable feature of Fig. 2C, in comparison with Fig. 2A, is the much wider range of L_β–L_o phase coexistence that is detected from the *sn*-2 [^{13}C]–C=O NMR signature as compared with that found from ^{2}H-NMR of the perdeuterated lipid chains. In the latter case, the phase boundaries are almost vertical and extend only up to a mole fraction $X \sim 0.22$ of cholesterol. In Fig. 2C, on the other hand, the upper phase boundary for L_β–L_o phase coexistence extends up to mole fractions of cholesterol $X > 0.4$. It should be emphasised that the evidence for L_β–L_o phase coexistence used in Fig. 2C is direct and based on detection of two-component NMR spectra. The implication is that the ^{13}C-NMR technique is better able to detect minor quantities of gel phase in the presence of a dominating L_o-phase than is the ^{2}H-NMR technique. Comparison of the relative lineshapes and spectral widths suggests that this is a reasonable interpretation. If this is true, it revises our concepts of the gel-phase region for the canonical binary phase diagram. These *sn*-2 [^{13}C]–C=O data appear to be ignored in contemporary considerations of phase diagrams that include liquid-ordered phases.

A second interesting feature of Fig. 2C is the rather indistinct nature of the horizontal three-phase line. Although this might be attributed to the relatively small number of data points, it does prompt questions as to the ubiquity of this canonical feature of the standard model for cholesterol-containing binary mixtures.

Fig. 2D shows a binary phase diagram for the 2,3-isomer of $(16:0)_2$PC (2,3-dipalmitoyl-*sn*-glycero-1-phosphocholine) with cholesterol [28]. The phase boundaries are determined solely from differential scanning calorimetry (DSC). The chain-melting phase boundary is defined by the position of the calorimetric peak, and achieving a homogeneous L_o-phase is defined by complete disappearance of the calorimetric transition. The lower boundary of the L_o-phase coexistence region at $X \approx 0.07$ is determined from the composition dependence of the width of the calorimetric peak.

Fig. 2E shows the phase diagram of $(16:0)_2$PC/cholesterol deduced from measurements of the permeability of acetic acid [29]. Data points

are given for the boundaries of the two-phase regions in the fluid and gel regimes, but not in the vicinity of the putative three-phase line. A significant feature is that boundaries of the single L_o-phase region are very similar to those in Fig. 2C, particularly that established by *sn*-2 [^{13}C]–C=O NMR, which does not agree with the nearly vertical boundary determined from ^{2}H-NMR measurements (Fig. 2A).

Fig. 2F shows the phase diagram of $(16:0)_2$PC/cholesterol, where the positions of the boundaries are deduced solely from differential scanning calorimetry [30]. A closed-loop region, designated here as L_α–L_o coexistence, was identified from the calorimetric measurements but, otherwise, phase boundaries such as those indicated by dashed lines in Fig. 2F were not identified in the original work.

3.2. Dimyristoylphosphatidylcholine $(14:0)_2$PC/cholesterol

Fig. 3 shows corresponding data for the shorter chain-length $(14:0)_2$PC lipid. That presented for the fluid phase in Fig. 3A is comparable to the EPR data for $(16:0)_2$PC in Fig. 2B (see [25]), but includes additional data from the biradical spin label (see [15]). It is also augmented by data from fluorescence photobleaching [31]; the high temperature part of the L_α-phase boundary corresponds to breaks in the behaviour of the lipid translational diffusion coefficient. The latter implies that the critical point, which was previously reported as occurring at 50 °C [25], lies at a higher temperature than would be predicted by the EPR data alone. The phase boundaries in the gel-phase regions of Fig. 3A, and the three-phase line, correspond to discontinuities in hyperfine splitting of spin-labelled 5-PC. Unlike in Fig. 2A for $(16:0)_2$PC, gel-phase coexistence (i.e., L_β–L_o) is not yet directly established for binary mixtures of $(14:0)_2$PC with cholesterol.

Fig. 3B presents data solely for the fluid phase from analysis of lifetime distributions of the fluorescence probe *trans*-parinaric acid. With increasing cholesterol content, a component of long fluorescence lifetime grows in. This is taken to represent the probe in liquid-ordered regions of the membrane. With a single adjustable parameter, the partition coefficient of *trans*-parinaric acid between the two fluid phases, agreement can be reached between the phase boundaries predicted from the fluorescence lifetime distributions and those given in Fig. 3A [32].

Fig. 3C presents one of the earliest experimental phase diagrams for a binary phospholipid mixture with cholesterol [33]. It is based on a variety of different spin-label EPR measurements, partly empirical. Although this lacks some of the phase boundaries appearing in later work, it is significant as the first proposal of fluid–fluid phase coexistence in the region above the well-defined three-phase line. The existence of both two-phase regions was established from the linearity of spin-label partitioning into the membrane, as predicted by the phase rule [33].

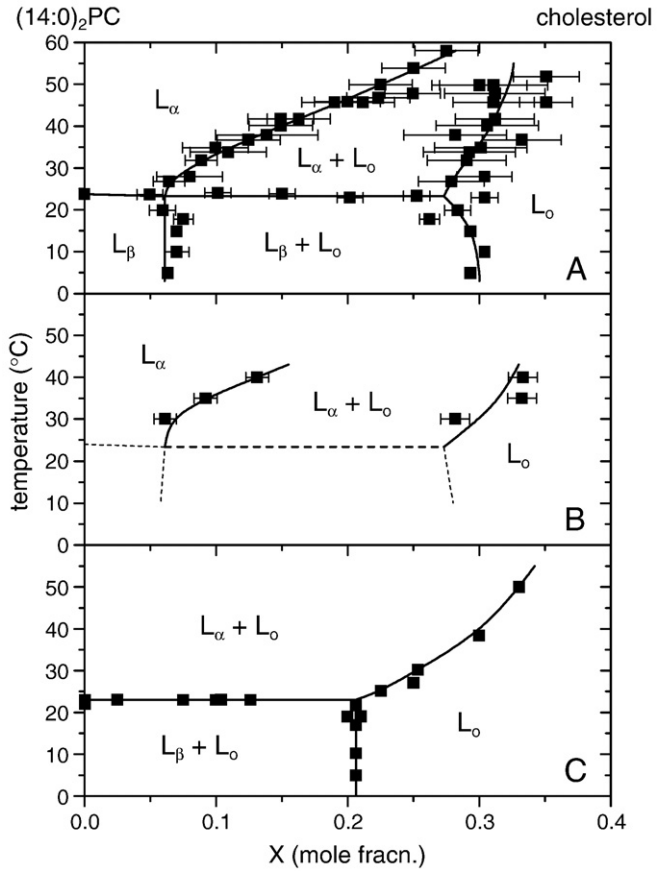

Fig. 3. Binary phase diagram for mixtures of dimyristoylphosphatidylcholine, $(14:0)_2$PC, with cholesterol dispersed in excess water. A. Data points from ref. [31]. Based on various methods, principally unpublished EPR results from M.B. Sankaram (see refs. [15,25], and cf. Fig. 2B), together with photobleaching. B. Data points from ref. [32], fluid phase only. Phase boundaries (symbols) deduced from analysis of fluorescence lifetime populations of *trans*-parinaric acid. C. Data points from ref. [33]. Phase boundaries deduced from a variety of spin-label EPR measurements. *X* is the mole fraction of cholesterol.

3.3. Dihexadecylphosphatidylcholine $(O\text{-}16:0)_2$PC/cholesterol

Fig. 4 shows binary phase diagrams for the ether-linked equivalent of dipalmitoylphosphatidylcholine in admixture with cholesterol. The dialkyl lipid differs from the diacyl lipid in that the chains from

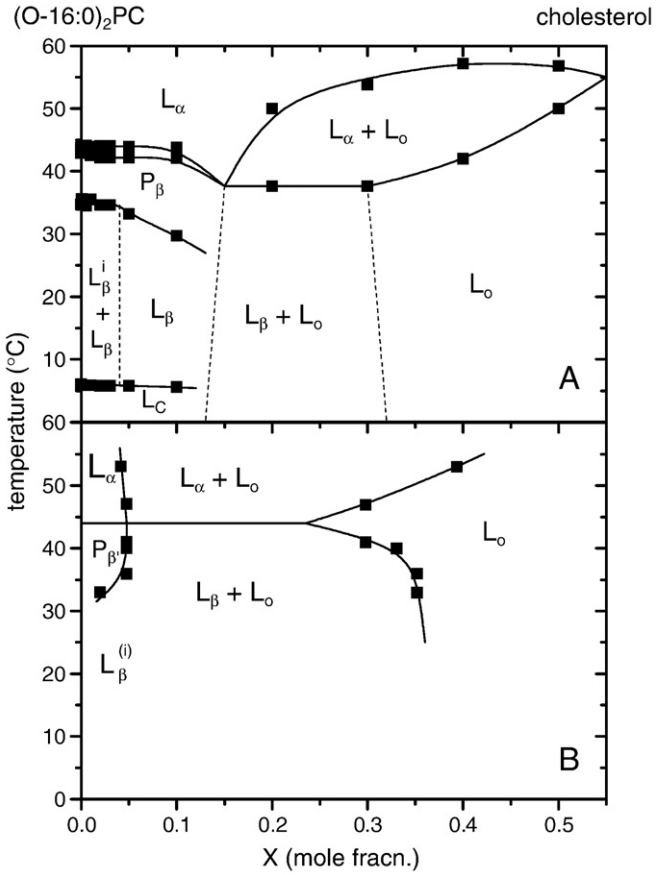

Fig. 4. Binary phase diagram for mixtures of dihexadecylphosphatidylcholine, $(O\text{-}16:0)_2$PC, with cholesterol, in excess water. A. Data points from ref. [35]. Phase boundaries (symbols) based on X-ray diffraction and DSC. B. Data points from ref. [29]. Based on compositional dependence of the permeability to acetic acid. L_β^i, is a fully interdigitated lamellar gel phase that is formed by $(O\text{-}16:0)_2$PC alone. L_c is a crystalline lamellar phase. *X* is the mole fraction of cholesterol.

apposing leaflets are completely interdigitated in the gel phase (see, e.g., ref. [34]), which is designated as L_{β}^{i}. Chain interdigitation is abolished at relatively low mole fractions of cholesterol, $X \sim 0.05$. Above this mole fraction, the gel phase is noninterdigitated.

Fig. 4A shows the (O-16:0)$_2$PC/cholesterol phase diagram determined from DSC measurements and X-ray diffraction [35]. Boundaries involving the L_o-phase are established only in the fluid regime (i.e., $L_\alpha + L_o$). Tentative boundaries involving $L_{\beta'}$–L_o phase coexistence are based on a putative three-phase line, but the small number of data points is insufficient to be definite on this point. The data of Fig. 4A could equally be interpreted without inclusion of a three-phase line (cf. the discussion of Fig. 2C given above). Fig. 4B shows the phase diagram deduced from measurements of the permeability of acetic acid [29]. Data points are given for the boundaries of the two-phase regions in both the fluid and gel regimes, but not in the vicinity of the putative three-phase line. This phase diagram is analogous to that given for the corresponding ester-linked lipid, (16:0)$_2$PC, in Fig. 2E. The position of the boundary between the fluid two-phase region and the single-phase L_o-region, corresponds well between Fig. 4A and B, but not for the boundary with the single-phase L_α-region.

3.4. Distearoylphosphatidylcholine (18:0)$_2$PC/cholesterol

Fig. 5 shows binary phase diagrams for mixtures of the longer chain-length phosphatidylcholine, (18:0)$_2$PC, with cholesterol. The data given in Fig. 5A are obtained primarily from ^{13}C-NMR and are directly comparable to those given for (16:0)$_2$PC in Fig. 2C. The binary phase diagram is essentially isomorphous to that of the shorter chain-length PC, and deviates in the same way from the current canonical model that is represented by Figs. 1, 2A and 3A. Similar comments apply here as were made regarding Fig. 2C.

Fig. 5B, for comparison, is a schematic rendering of part of a phase diagram, which is based on unpublished spin-label data from M.B. Sankaram [25], and is analogous to Fig. 2B for (16:0)$_2$PC. The data, in fact, extend to higher temperatures than those given in Fig. 5B, with a reported critical point at ca. 85 °C [25]. Inverted triangles in Fig. 5B represent the percolation thresholds at which complete recovery of fluorescence from a phospholipid probe is obtained after photobleaching [36]. Below these points, the fluid domains are discontinuous; percolation occurs when connectivity between domains is achieved. The photobleaching experiments therefore provide direct evidence for $L_{\beta'}$–L_o phase coexistence in the gel-phase regime. Note also that the trend in the percolation points in Fig. 5B is more consistent with a tilted L_o-phase boundary than with a vertical one (cf. Fig. 5A).

Fig. 5C shows a recent phase diagram for (18:0)$_2$PC/cholesterol that is constructed solely on the basis of DSC measurements [37]. In the original publication, emphasis was put on a complex eutectic behaviour at temperatures above T_m for (18:0)$_2$PC and relatively low cholesterol contents ($X \leq 0.15$) that was attributed to particular regular distributions of cholesterol in the gel phase. Above this are regions of coexistence with the L_o-phase, which was suggested to extend up to cholesterol mole fractions of $X \leq 0.5$.

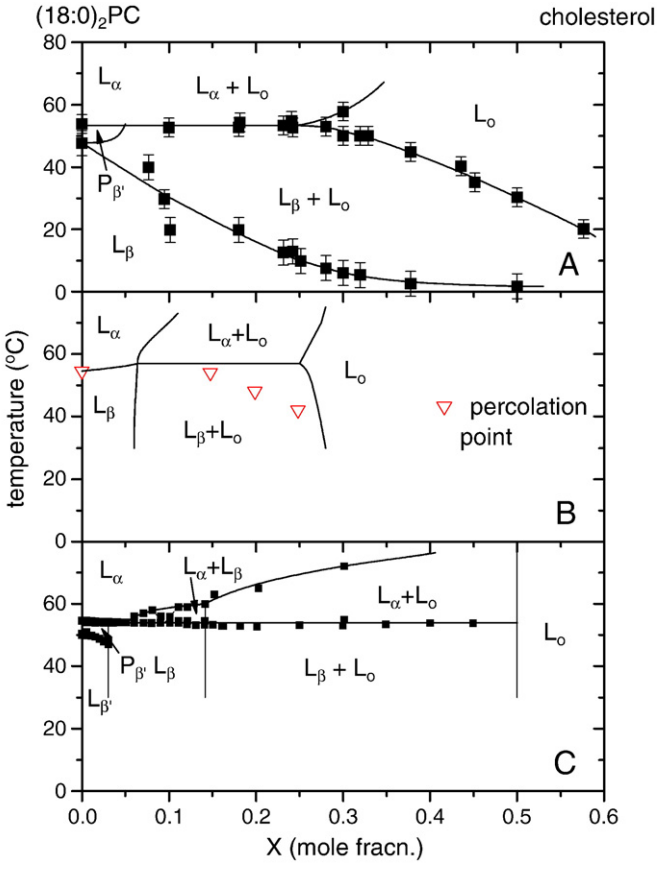

Fig. 5. Binary phase diagram for mixtures of distearoylphosphatidylcholine, (18:0)$_2$PC, with cholesterol, in excess water. A. Specifically deuterated or *sn*-2 [^{13}C]–C = O labelled (18:0)$_2$PC. Data points from ref. [26]. Phase boundaries below the chain-melting temperature of (18:0/[1-^{13}C]18:0)PC are deduced from ^{13}C-NMR. B. Adapted from ref. [36]. Phase boundaries, summarised by continuous lines, are from EPR spectra of spin-labelled PC (see ref. [25]). Inverted triangles mark percolation points from photobleaching recovery. C. Data points from ref. [37]. Deduced from DSC measurements. *X* is the mole fraction of cholesterol.

3.5. Diheptadecanoylphosphatidylcholine (17:0)$_2$PC/cholesterol

Fig. 6 shows the binary phase diagram for mixtures of diheptadecanoylphosphatidylcholine, (17:0)$_2$PC, with cholesterol [38]. The phase boundaries are deduced solely from DSC endotherms, and are directly comparable to Fig. 5C which was obtained for (18:0)$_2$PC by the same workers. Again, eutectic/peritectic behaviour at cholesterol mole fractions $X \leq 0.15$ was attributed to complex formation in the gel phase, with $L_{\beta'}$–L_o and L_α–L_o phase coexistence at cholesterol contents above this. In this case, the phase coexistence was suggested to extend only up to $X \leq 0.3$.

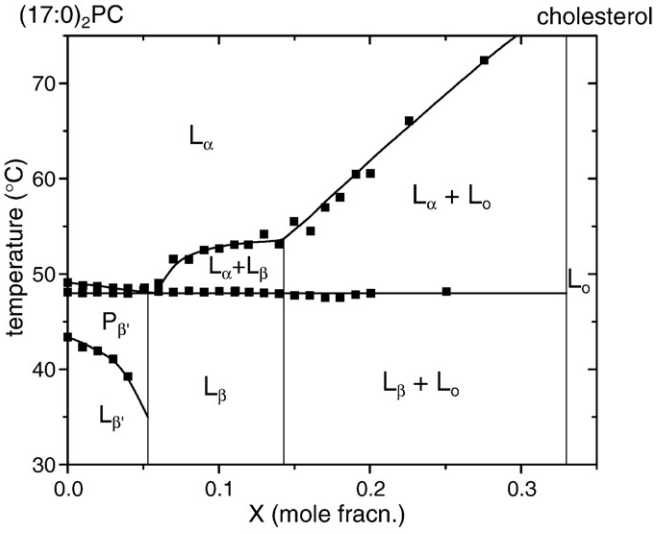

Fig. 6. Binary phase diagram for mixtures of diheptadecanoylphosphatidylcholine, (17:0)$_2$PC, with cholesterol in excess water. Data points from ref. [38]. Deduced from DSC measurements. *X* is the mole fraction of cholesterol.

3.6. 1-palmitoyl-2-oleoylphosphatidylcholine (16:0/18:1cΔ^9)PC/cholesterol

Fig. 7 shows binary phase diagrams for mixtures of palmitoyl-oleoylphosphatidylcholine with cholesterol. The chain-melting temperature of this unsaturated lipid lies somewhat below 0 °C. Fig. 7A gives data from ^{2}H-NMR of the perdeuterated palmitoyl chain, which is analogous to that given for the saturated $(16:0)_2$PC in Fig. 2A. Again, L_β–L_o phase separation is detected in the low-temperature region, but in contrast to Fig. 2A, no conclusive evidence, either direct or indirect, is found from the ^{2}H-NMR spectra for phase boundaries or L_α–L_o phase separation in the fluid regime. There is, however, a rather clear horizontal three-phase line at −7 °C, which implies L_α–L_o phase coexistence at temperatures immediately above this. Interestingly, the upper boundary of L_β–L_o phase coexistence in Fig. 7A depends less steeply on cholesterol content than do those for other systems investigated by ^{2}H-NMR (cf. Figs. 1, 2A, 8A and 8B).

Panels B and C of Fig. 7 give data that are restricted to the fluid regime, where phase boundaries are deduced by using fluorescence probes. Fig. 7B presents data derived from fluorescence lifetimes of *trans*-parinaric acid, and Fig. 7C that from the dependence of the steady-state fluorescence polarisation of diphenylhexatriene and lifetime-weighted quantum yield of *trans*-parinaric acid on composition. The data in Fig. 7B is directly comparable to that from the saturated lipid $(14:0)_2$PC which is given in Fig. 3B. In this case, however, the partition coefficient of *trans*-parinaric acid between the two phases was determined by independent fluorimetric titrations [32]. Therefore, unlike the situation in Fig. 3B, the phase diagram is determined entirely from fluorescence measurements alone. The phase boundaries for fluid–fluid phase separation in Fig. 7B are extended to meet a notional three-phase line at −3 °C. It is clear that the fluid-phase data extrapolate to L_β–L_o phase separation at considerably lower cholesterol contents than is depicted in Fig. 7A. Although both sets of fluorescence data are interpreted in favour of L_α–L_o phase coexistence, they differ considerably in the positions predicted for the phase boundaries. The extrapolations in Fig. 7C to a three-phase line at −3 °C are much closer to the experimental determinations of the L_β–L_o coexistence region in Fig 7A than are those of Fig 7B.

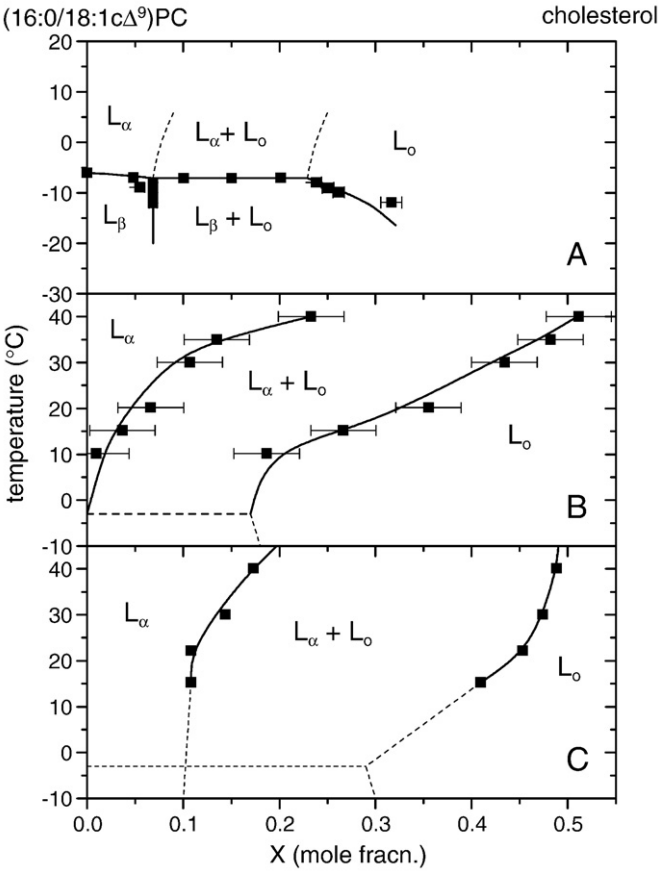

Fig. 7. Binary phase diagram for mixtures of 1-palmitoyl-2-oleoylphosphatidylcholine, (16:0/18:1cΔ^9)PC, with cholesterol, in excess water. A. (d_{31}-16:0/18:1cΔ^9)PC with perdeuterated palmitoyl chain. Data points from ref. [5]. Phase boundaries (symbols) determined from 2-component ^{2}H-NMR spectra, in the gel phase only. B. Normal protiated (16:0/18:1cΔ^9)PC. Data points from ref. [32]. Phase boundaries (symbols; fluid phase only) deduced from distribution of fluorescence lifetimes of *trans*-parinaric acid. C. Normal protiated (16:0/18:1cΔ^9)PC. Data points from ref. [55]. Phase boundaries (symbols; fluid phase only) are determined from fluorescence polarisation of diphenylhexatriene and lifetime-weighted quantum yield of *trans*-parinaric acid. *X* is the mole fraction of cholesterol.

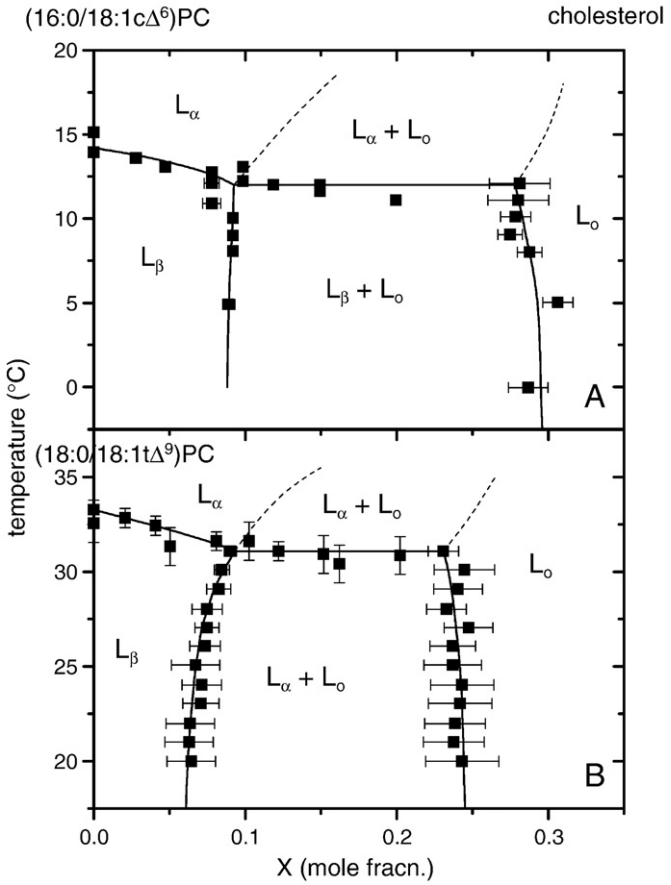

Fig. 8. Binary phase diagram for mixtures of 1-palmitoyl-2-petroselinoylphosphatidylcholine, (16:0/18:1cΔ^6)PC, or 1-stearoyl-2-elaidoylphosphatidylcholine, (16:0/18:1tΔ^9)PC, with cholesterol dispersed in water. A. (d_{31}-16:0/18:1cΔ^6)PC with perdeuterated palmitoyl chain. Data points from ref. [5]. B. (d_{35}-18:0/18:1tΔ^9)PC with perdeuterated stearoyl chain. Data points from ref. [45]. Phase boundaries (symbols) in both cases are determined from 2-component ^{2}H-NMR spectra, solely in the gel phase; chain-melting phase boundaries are also from DSC. *X* is the mole fraction of cholesterol.

3.7. 1-palmitoyl-2-petroselinoylphosphatidylcholine (16:0/18:1cΔ^6)PC/cholesterol, and 1-stearoyl-2-elaidoylphosphatidylcholine (18:0/18:1tΔ^9)PC/cholesterol

Fig. 8 shows the binary phase diagrams of two further unsaturated phosphatidylcholines mixed with cholesterol. As in Figs. 2A and 7A, the data on L_β–L_o phase separation are obtained from ^{2}H-NMR spectra of perdeuterated chains. This is combined with DSC measurements for the chain-melting behaviour, i.e., boundaries involving L_β–L_α

conversions. In contrast to (16:0/18:1cΔ^9)PC, the chain-melting temperatures of (16:0/18:1cΔ^6)PC and (18:0/18:1tΔ^9)PC lie above 0 °C, as for the saturated lipid (16:0)$_2$PC. Nonetheless, as for (16:0/18:1cΔ^9)PC, definite evidence for phase separation in the fluid regime was not obtained. Phase separation is detected from two-component ^{2}H-NMR spectra in the low-temperature regime and the upper boundary of this L_β–L_o phase coexistence region approximates to a horizontal three-phase line. Again, the latter implies L_α–L_o phase coexistence immediately above this boundary but direct evidence from the NMR spectra is lacking.

4. Sphingomyelin-cholesterol mixtures

4.1. Sphingomyelin SM(d18:1/n:0)/cholesterol

The phase behaviour of binary mixtures of sphingomyelin, SM (d18:1/*n*:0), with cholesterol is of especial interest because sphingolipids are thought to be the high-melting lipid component responsible for lipid raft formation in cholesterol-containing cell membranes. [*Note*: d18:1 ≡ sphing-4-enine ≡ (2*S*,3*R*,4*E*)-2-amino-4-octadecene-1,3-diol (sphingosine).] Fig. 9 gives the binary phase diagrams for three different *N*-acyl sphingophosphocholines mixed with cholesterol.

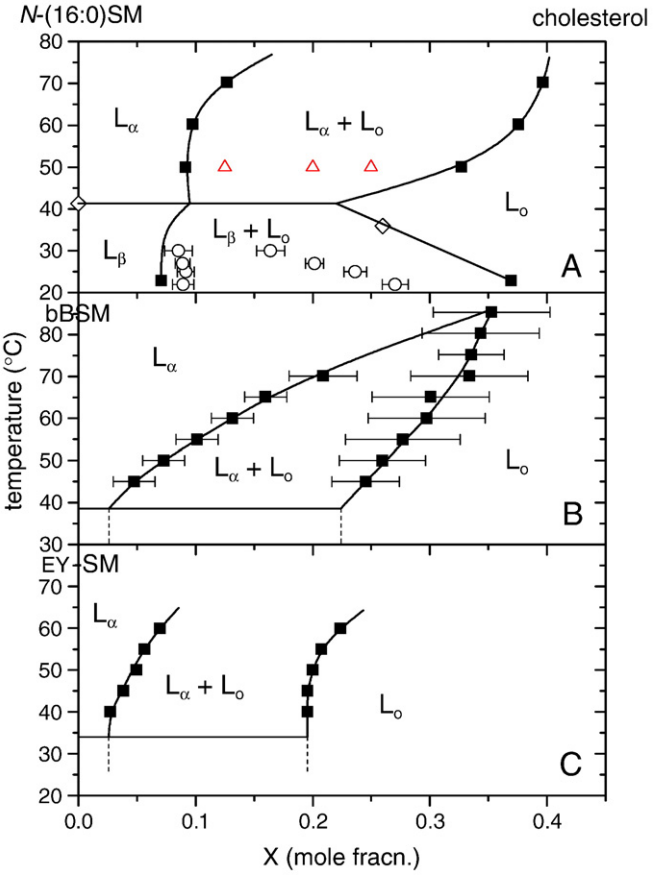

Fig. 9. Binary phase diagram for mixtures of sphingomyelin, SM(d18:1/*n*:0) with cholesterol in excess water. A. *N*-palmitoylsphingomyelin SM(d18:1/16:0). Data points from ref. [55]. Phase boundaries (squares and diamonds) in the fluid phase determined by fluorescence polarisation of diphenylhexatriene and in the gel phase by fluorescence quenching with spin-labelled stearic acid. Open triangles are points of L_α–L_o phase coexistence established by two-component EPR spectra, and open circles are L_β–L_o phase boundaries established similarly [16]. B. Bovine brain sphingomyelin, predominantly SM(d18:1/18:0) and SM(d18:1/24:1cΔ^{15}). Data points from ref. [25]. Phase boundaries (symbols; fluid phase only) based on composition dependence of outer hyperfine splittings from spin-labelled phosphatidylcholine. C. Egg yolk sphingomyelin, predominantly SM(d18:1/16:0). Data points from ref. [47]. Phase boundaries are located from the sharp linear decrease in lipid translational diffusion with increasing cholesterol content in the $L_\alpha + L_o$ coexistence region. *X* is the mole fraction of cholesterol.

Fig. 9A shows the phase diagram for *N*-palmitoylsphingomyelin, SM(d18:1/16:0), that is established in the fluid regime from the steady-state fluorescence polarisation of diphenylhexatriene and, in the gel regime, from fluorescence-quenching by spin-labelled stearic acid. Data in the latter region is extremely sparse and no information is given on the phase boundaries between gel and fluid regions, which are simply indicated schematically in Fig. 9A. For this system, direct evidence for phase coexistence in the $L_\alpha + L_o$ region has been provided by two-component EPR spectra of spin-labelled sphingomyelin (and phosphatidylcholine) [16], as indicated by open triangles in the figure. Open circles indicate phase boundaries deduced from two-component EPR spectra in the $L_\beta + L_o$ region [16]. These are calculated with the assumption of equipartitioning of the spin-labelled phospholipid between the two phases (see Eq. (3)), which experimentally seems to be a reasonable approximation [16,39,40]. Note that inhomogeneities, and hence two-component spectra, potentially could arise from differential lipid solubilities in the organic solvent that is used to prepare the binary mixtures, but for PC–cholesterol or SM–cholesterol mixtures this is unlikely to be a serious issue at cholesterol contents well below the solubility limit (see, e.g., [41]).

Fig. 9B shows the phase diagram for sphingomyelin from bovine brain which has predominantly stearoyl and nervonyl *N*-acyl chains (i.e., SM(d18:1/18:0) and SM(d18:1/24:1cΔ^{15})). The data here is restricted to the fluid regime and the boundaries of the L_α–L_o phase coexistence region are determined indirectly from the dependence of hyperfine splittings from spin-labelled lipids on cholesterol content. In this phase diagram, a critical point is suggested at ca. 86 °C and mole fraction of cholesterol $X \sim 0.35$. Above this temperature, the outer hyperfine splitting changes monotonically with cholesterol content.

Fig. 9C gives the phase diagram for sphingomyelin from egg, the *N*-acyl chains of which are predominantly palmitoyl (i.e., SM(d18:1/16:0)). The phase boundaries determined are restricted to the fluid regime and are obtained from pulse-gradient NMR measurements of lipid translational diffusion as a function of composition. Fast exchange between domains of submicron size ensures a linear dependence on mole fraction of cholesterol throughout the fluid coexistence region and, therefore, the phase coexistence and location of phase boundaries are determined with reasonable precision [42]. The phase boundaries in Fig. 9C differ considerably in shape from the other two cases, particularly that with the L_o single-phase region, which is extremely steep with little evidence for coalescence with the L_α boundary to reach a critical point.

5. Asymmetric phosphatidylcholine-sterol mixtures

5.1. 1-stearoyl-2-decanoylphosphatidylcholine (18:0/10:0)PC/sterol

Fig. 10 gives partial phase diagrams for mixtures of the asymmetric-chain phosphatidylcholine (18:0/10:0)PC with either cholesterol (Fig. 10A) or dehydroergosterol (Fig. 10B). For this phospholipid, the *sn*-2 chain is considerably shorter than the *sn*-1 chain, which results in formation of a mixed interdigitated gel phase and also affects its mixing behaviour with cholesterol. Data were obtained by calorimetry and no attempt was made to identify phase coexistence regions of the L_β–L_o or L_α–L_o type. Indeed, the calorimetric data suggest that no such regions are present. The two sterols induce a progressive decrease in temperature and increase in width of the calorimetric peak. A narrow region of gel–fluid coexistence (presumably $L_\beta + L_\alpha$) is detected corresponding to the chain-melting event. These phase boundaries move to progressively lower temperatures with increasing cholesterol content. Up to mole fractions of sterol $X \geq 0.2$, there is no indication of any horizontal

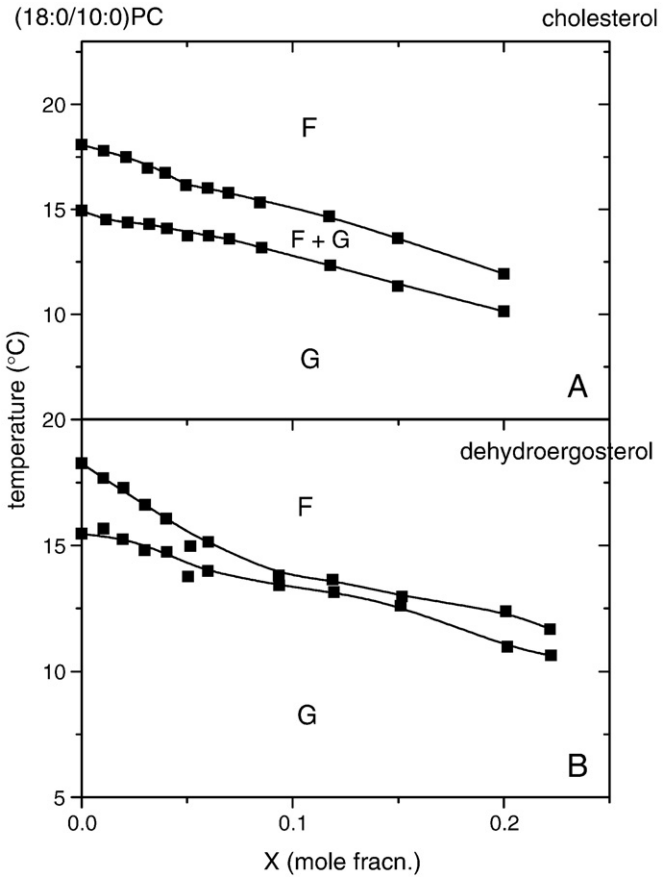

Fig. 10. Phase diagram for binary mixtures of asymmetric-chain phosphatidylcholine (18:0/10:0)PC with sterols dispersed in excess water. A. (18:0/10:0)PC and cholesterol. Data points from ref. [59] obtained by DSC. B. (18:0/10:0)PC and dehydroergosterol. Data points from ref. [60] obtained by DSC. F and G are fluid- and gel-phase regions, respectively. *X* is the mole fraction of sterol.

section of the phase boundary that might indicate a line of three-phase coexistence as in Figs. 2A, 3A, 7A, 8A and 8B. At mole fractions of sterol above $X \sim 0.25$–0.27, the calorimetric transition is entirely abolished. Qualitatively, the results obtained with dehydroergosterol (Fig. 10B) are extremely similar to those obtained with cholesterol (Fig. 10A).

6. Phosphatidylethanolamine-cholesterol mixtures

6.1. Dipalmitoylphosphatidylethanolamine (16:0)$_2$PE/cholesterol

Fig. 11 presents a partial phase diagram for binary mixtures of the saturated phosphatidylethanolamine, (16:0)$_2$PE, with cholesterol. Data are given from both *sn*-2 [^{13}C]–C=O NMR and ^{2}H-NMR of the isotopically labelled phospholipid (cf. Figs. 2C and 5B), and also from differential scanning calorimetry [6]. The apparent phase boundaries from the two methods, NMR and DSC, do not coincide. This was attributed to the low cooperativity in cholesterol-containing systems, which results in broadened DSC endotherms. Two-component NMR spectra clearly identify phase coexistence in the region designated $L_\beta + L_o$, whereas only single-component spectra are found in the region designated L_o. No evidence for fluid–fluid phase coexistence (i.e., $L_\alpha + L_o$) was found from the NMR spectra, but the data for completion of chain-melting from DSC suggest the presence of a three-phase line. Overall, the phase diagram resembles those for phosphatidylcholines (Figs. 2C and 5A) determined by the same NMR methods.

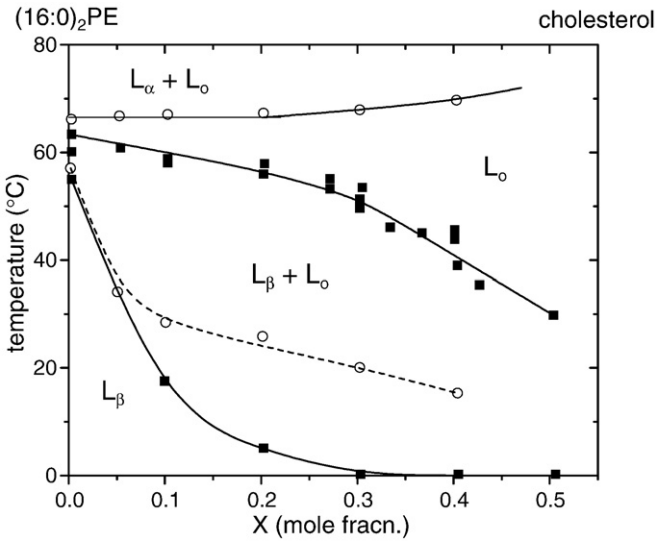

Fig. 11. Binary phase diagram for mixtures of dipalmitoylphosphatidylethanolamine (16:0)$_2$PE with cholesterol in excess water. Data from ref. [6]. Boundaries are from NMR spectroscopy (solid lines and solid symbols) and from DSC (dashed lines and open symbols). Phases assigned are those enclosed by both sets of boundaries. *X* is the mole fraction of cholesterol.

6.2. Dielaidoylphosphatidylethanolamine (18:1tΔ^9)$_2$PE/cholesterol, and 1-palmitoyl-2-oleoylphosphatidylethanolamine (16:0/18:1cΔ^9)PE/cholesterol

Panels A and B of Fig. 12 present partial phase diagrams for binary mixtures of unsaturated phosphatidylethanolamines, (18:1tΔ^9)$_2$PE or (16:0/18:1cΔ^9)PE, with cholesterol. Phase boundaries are determined by DSC, with some additional supporting data from infrared spectroscopy in the case of (16:0/18:1cΔ^9)PE. The possibility of formation of liquid-ordered phases was not considered specifically in these cases. The work concentrated on the effects of cholesterol on chain-melting of the phosphatidylethanolamine lipids, and on the transition from a lamellar (L_α) phase to an inverted hexagonal (H_{II}) phase at higher temperatures in the fluid regime.

In Fig. 12A for dielaidoylphosphatidylethanolamine, (18:1tΔ^9)$_2$PE, approximately horizontal phase boundaries in the region of chain-melting at ~37 °C and of lamellar-hexagonal transition at ~60 °C extend over the range of cholesterol mole fractions $X \sim 0.1$–0.35. This suggests coexistence of $L_\beta + L_o$ phases and of $L_\alpha + L_o$ phases in the regions below and above the horizontal phase boundary at ~37 °C, respectively. The horizontal phase boundary at ~60 °C suggests coexistence of two fluid lamellar phases with the single H_{II}-phase in the high temperature regime, and thus is consistent with the assignment of the $L_\alpha + L_o$ phase coexistence region as indicated. The phase boundary in the low-temperature regime, suggested tentatively as being between the L_β gel phase and $L_\beta + L_o$ coexistence region, differs considerably from those in the canonical standard model established for phosphatidylcholines by ^{2}H-NMR, i.e., Figs. 1, 2A, 7A, 8A and 8B. It does, however, bear strong similarities to the corresponding phase boundaries established by *sn*-2 [^{13}C]–C=O NMR for (16:0)$_2$PC and (18:0)$_2$PC (see Figs. 2C and 5A). It should be emphasised that the assignments of L_o=phases that are suggested here on the basis of analogy with the PC systems were not part of the original analysis [43].

The corresponding data for binary mixtures of the mixed-chain unsaturated phosphatidylethanolamine, (16:0/18:1cΔ^9)PE in Fig. 12B do not display phase boundaries with such clear horizontal segments as in Fig. 12A. Thus, they are not amenable to a similar analysis, because they lack definite analogies with the standard model for phosphatidylcholine. Instead, it is possible that the chain-melting and lamellar-

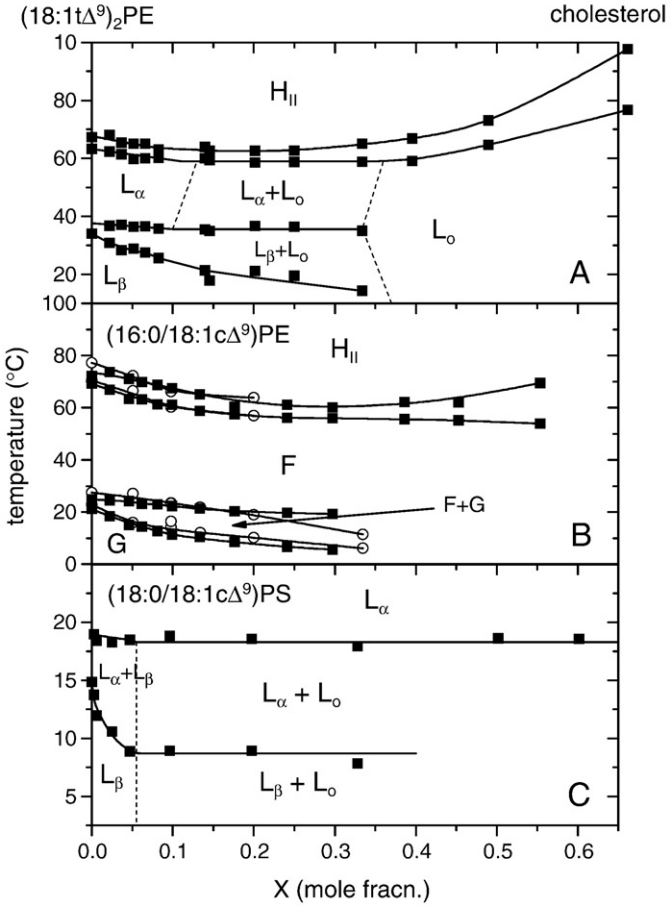

Fig. 12. Binary phase diagrams for mixtures of phosphatidylethanolamine or phosphatidylserine with cholesterol in excess water. A. dielaidoylphosphatidylethanolamine $(18{:}1t\Delta^9)_2$PE. Data points from ref. [43] obtained by differential scanning calorimetry (DSC). B. 1-palmitoyl-2-oleoylphosphatidylethanolamine $(16{:}0/18{:}1c\Delta^9)$PE. Data points from ref. [43] (solid symbols) obtained by DSC, and from ref. [61] (open symbols) obtained by DSC and infrared spectroscopy. C. 1-stearoyl-2-oleoylphosphatidylserine $(18{:}0/18{:}1c\Delta^9)$PS. Data points from ref. [44] obtained by DSC. X is the mole fraction of cholesterol.

hexagonal phase boundaries change progressively with increasing cholesterol content, rather like the situation for chain-melting of the asymmetric phosphatidylcholine (18:0/10:0)PC (cf. Fig. 10). In this case, phosphatidylethanolamine may not interact with cholesterol in a manner similar to that of the corresponding phosphatidylcholine (cf. Fig. 7).

7. Phosphatidylserine-cholesterol mixtures

7.1. 1-stearoyl-2-oleoylphosphatidylserine, $(18{:}0/18{:}1c\Delta^9)$PS/cholesterol

Fig. 12C shows the binary phase diagram for mixtures of the anionic lipid $(18{:}0/18{:}1c\Delta^9)$PS with cholesterol. A moderate anionic strength provided by 0.15 M NaCl serves partially to screen strong electrostatic repulsions in this system. The data for this asymmetric unsaturated lipid reported in Fig. 12C are derived from differential scanning calorimetry and refer to the chain-melting behaviour. Assignments to liquid-ordered phases were not made. The phase boundaries of the $L_\alpha + L_\beta$ chain-melting region decrease with increasing cholesterol content up to a mole fraction $X \sim 0.05$. Beyond this they remain essentially horizontal up to a mole fraction of cholesterol, $X \sim 0.3$. In analogy with the discussion of phosphatidylcholine systems, this could suggest the presence of phase coexistence with a liquid-ordered phase as indicated in the figure. However, only a single bilayer repeat spacing is observed with low-angle X-ray diffraction in this region [44]. It should be noted that a mole fraction of $X \sim 0.3$ approximates the maximum solubility of cholesterol in $(18{:}0/18{:}1c\Delta^9)$PS membranes, because beyond this a thermotropic transition is observed from pure phase-separated cholesterol. A small X-ray diffraction peak from crystalline cholesterol is detected even at $X \sim 0.2$ [44].

8. Discussion

8.1. Nonuniversal paradigm?

Comparison of the binary phase diagrams in Fig. 12 for phosphatidylethanolamines and phosphatidylserines with corresponding ones for phosphatidylcholines that are given in the preceding figures, suggests clear differences in the interactions of these two lipids with cholesterol from those for the much more extensively studied phosphatidylcholines. Comparison with the phosphatidylcholine/cholesterol phase diagrams, particularly with respect to the appearance of putative three-phase lines, suggests that liquid-ordered phases might be formed with certain phosphatidylethanolamine and phosphatidylserine lipids, but this is by no means certain. It should be emphasised that there is no direct evidence for $L_\alpha + L_o$ or $L_\beta + L_o$ phase coexistence for the PE or PS systems of Fig. 12A and 12C. The appropriate experiments have yet to be done with these lipid species.

The phase behaviour of the highly asymmetric phosphatidylcholine, (18:0/10:0)PC, mixed with cholesterol is very different from that for binary mixtures with symmetric phosphatidylcholines (see Fig. 10). There is no suggestion from the calorimetric evidence for the formation of liquid-ordered phases. However, this system has not been studied by ^{2}H-NMR, which has proved diagnostic in the case of the symmetric phosphatidylcholines.

8.2. L_o-phase coexistence

Although phosphatidylcholine (or sphingomyelin) systems provide evidence for liquid-ordered phases and their coexistence with the gel or fluid phases, there is not complete agreement amongst the various phase diagrams determined for binary mixtures of cholesterol with the same phosphatidylcholine species. There is a reasonable consensus as to the coexistence of gel and liquid-ordered phases ($L_\beta + L_o$) in phosphatidylcholine–cholesterol mixtures. Direct evidence for this comes from two-component NMR spectra of isotopically labelled lipids, either deuterated chains [4,5,45] or ^{13}C-labelled *sn*-2 carbonyls [26]. Regarding the latter, it is worthwhile to reemphasise that it provides evidence for a more extended range of L_β–L_o phase coexistence (Figs. 2C and 5A) than is depicted by the current canonically accepted quasi-vertical phase boundaries deduced from ^{2}H-NMR. As reviewed recently [10], there is far less consensus, however, regarding L_α–L_o phase coexistence than for the L_β–L_o case, and only rather limited data that demonstrates this phase coexistence directly in binary lipid mixtures with cholesterol. Currently, I am aware of only three clear instances, those already mentioned previously. These are the observations of two-component EPR spectra of spin-labelled lipids in mixtures of SM(d18:1/16:0) with cholesterol over a reasonably wide composition range [16], or of $(16{:}0)_2$PC with cholesterol [15], and of two-component ^{2}H-NMR spectra of chain-perdeuterated $(d_{31}\text{-}16{:}0)_2$PC in mixtures with cholesterol at temperatures above the chain-melting region [17].

8.3. Domain size

A consideration of the influence of spectroscopic timescale on the observation of two-component spectra is, perhaps, appropriate here. Whether two-component spectra are observed in a magnetic resonance experiment depends on the size of the domains, the

translational diffusion coefficient (D_T) of the lipids, and the difference ($\delta\Delta\omega$) in spectral position or splitting for lipids in the L_α-and L_o-phases. For two-dimensional Brownian diffusion, the mean-square distance travelled by a lipid molecule in time interval τ is:

$$\langle r^2\rangle = 4D_T\tau \tag{4}$$

where typical diffusion coefficients are $D_T \sim 10\,\mu m^2\,s^{-1}$ in L_α-phases and a factor of two lower in L_o-phases [46,47]. For spectra from adjacent domains not to be averaged over the time span τ requires that exchange is slow on the magnetic resonance timescale (see, e.g., ref. [48]):

$$\tau^{-1} \ll \delta\Delta\omega \tag{5}$$

where τ^{-1} represents the average exchange rate. In the ^{2}H-NMR spectra of deuterated lipids, the smallest difference in quadrupole splittings between the L_α-and L_o-phases is: $\delta\Delta\omega_Q \sim 6\times10^3$ rad s^{-1}, for the chain terminal methyls, and the largest difference is: $\delta\Delta\omega_Q \sim 7\times10^4$ rad s^{-1}, for the chain order-parameter plateau region. To observe two-component terminal methyl ^{2}H-NMR spectra therefore requires domain diameters considerably larger than 100–200 nm, whereas, for two-component spectra in the order-parameter plateau region, domain diameters only need to be considerably larger than 30–50 nm. For spin-label EPR, on the other hand, the resolved splitting between spectra from the L_α-and L_o-phases in SM(d18:1/16:0)-cholesterol mixtures is $\delta\Delta\omega_{EPR} \sim 7\times10^7$ rad s^{-1} [16] and, therefore, two-component spectra are expected irrespective of the domain size. Both L_α-and L_o-phases give the quasi-isotropic ^{13}C-NMR signature from *sn*-2 carbonyls and, therefore, this method cannot be used to detect fluid–fluid phase coexistence. For the gel phase, the minimum difference in chemical shift anisotropy from the L_o-phase is: $\delta\Delta\omega_{csa} \sim 1.7\times10^4$ rad s^{-1}, at the field strength used, and the maximum is twice this. However, translational diffusion coefficients in the gel phase are 10^3 times smaller than in the fluid phase [49]. Therefore, two-component spectra are expected even with the smallest domains. In fact, the diameter of the gel-phase domains has been estimated as ~18 nm, from lifetime broadening of the isotropic ^{13}C-NMR line of the L_o-phase [26]. For comparison, in a pulse field-gradient NMR experiment, the timescale is determined by the diffusion time interval, Δ, between gradient pulses, with a typical minimum value of $\Delta = 50$ ms [50,51]. From Eq. (4), this corresponds to a minimum domain diameter of 1.5–3 μm for resolving two components of translational diffusion by pulse-gradient NMR. For optical resolution of domains by fluorescence microscopy the lower limit is ~300 nm [52]. Thus, for observation of phase coexistence, only spin-label EPR, and solid-state NMR in the gel phase region, are expected not to be limited by domain size.

8.4. Phase boundaries: indirect methods

In view of the above, it is worthwhile to review the indirect methods used to establish the phase boundaries in the binary systems, with a critical eye on whether these really support the concept of coexistence of L_α-and L_o-phases.

Translational diffusion rates are approximately two-fold slower in L_o-phases than in the corresponding L_α-phases at the same temperature. In a pulsed field-gradient NMR determination of translational diffusion, fast exchange takes place between L_α-and L_o-domains in a region of phase separation, if the domains are of submicron size [42] (cf. section 8.3). In the two-phase region, the diffusion coefficient, D_T ($L_\alpha + L_o$), that is measured then depends linearly on the fractional population, f_{Lo}, of L_o-phase:

$$D_T(L_\alpha + L_o) = (1-f_{Lo})D_T(L_\alpha) + f_{Lo}D_T(L_o) \tag{6}$$

which, according to the phase rule (Eq. (2)), in turn is linearly dependent on the mole fraction, X, of cholesterol. Within the single-phase regions, the diffusion coefficient depends much less on cholesterol content [47]. Therefore, under fast-exchange conditions, the linear dependence is a suitable indicator of phase coexistence (as used for Fig. 9C). The assumption is that domain boundaries are not a significant portion of the whole and that fluid domains do not function as obstacles, other than by changing the intrinsic diffusion rate. A more general treatment for composites is given in ref. [31]. Note that the diffusion coefficient of intrinsic lipid components, not of probes, is measured in the pulsed field-gradient NMR experiment.

It is important to note that, whereas discontinuities indicating L_α–L_o phase boundaries were found in the sphingomyelin–cholesterol system, a completely linear dependence of the translational diffusion coefficient on mole fraction of cholesterol was found in binary mixtures with dioleoyl phosphatidylcholine and with palmitoyl-oleoyl phosphatidylcholine [47], and also with stearoyl-oleoyl, stearoyl-linoleoyl and stearoyl-arachidonyl phosphatidylcholines [53], at all cholesterol contents. This suggests the formation of a homogeneous phase, at temperatures of 21 °C and above, in these binary mixtures of unsaturated phosphatidylcholines with cholesterol. The upper phase boundary (i.e., with the L_o single-phase region) is detected from pulsed field-gradient NMR measurements of translational diffusion on binary mixtures of dimyristoyl phosphatidylcholine with cholesterol, but no clear lower boundary was distinguished (with an L_α single-phase region) [47]. The latter is, however, indicated by photobleaching measurements of translation diffusion at 26 °C [49]. Discontinuities also are detected by pulsed field-gradient NMR in the cholesterol dependence of the translational diffusion coefficient of dipalmitoyl phosphatidylcholine in the fluid-phase region of binary mixtures (supplementary material in ref. [54]), although the positions do not entirely coincide with estimates of the phase boundaries by other means.

The linear dependence of the fluorescence anisotropy, $\langle r\rangle$, of diphenyl hexatriene on cholesterol content (used for Figs. 7C, 9A [55]) is less direct because the definition of $\langle r\rangle$ involves a normalisation by the fluorescence intensity:

$$\langle r\rangle = \frac{I_{/\!/} - I_\perp}{I_{/\!/} + 2I_\perp} \tag{7}$$

where $I_{//}$ and $I_\perp$ are the fluorescence intensities with polarisation parallel and perpendicular, respectively, to the plane of polarisation of the exciting light. If it is assumed that the extinction coefficient for excitation and the ratio of the fluorescence intensity at the wavelength of emission to the total fluorescence intensity are the same in the two phases, then the fluorescence anisotropy measured in the region of $L_\alpha + L_o$ phase coexistence is related to the fraction, f, of probe in the L_o phase by [55]:

$$\langle r\rangle = \frac{f\Phi_{Lo}\langle r_{Lo}\rangle + (1-f)\Phi_{L\alpha}\langle r_{L\alpha}\rangle}{f\Phi_{Lo} + (1-f)\Phi_{L\alpha}} \tag{8}$$

where $\langle r_{Lo}\rangle$ and Φ_{Lo} are the fluorescence anisotropy and the quantum yield, respectively, of the probe in the L_o phase, and similarly for the probe in the L_α phase. Thus it requires that the fluorescence quantum yield does not change between phases ($\Phi_{Lo} = \Phi_{L\alpha}$) for $\langle r\rangle$ to depend linearly on f (Eq. (8)). Additionally, equal partitioning of the probe between the two phases is required for f to be linearly related to the mole fraction, X, of cholesterol (see Eq. (3)) (see also [56]). Departures from these conditions could affect the sensitivity and accuracy with which phase boundaries can be detected.

Methods based on the fluorescence lifetime distributions of *trans*-parinaric acid (Figs. 3B, 7B [32]) reflect the phase coexistence in so far as the different lifetime populations correspond to the probe in the different phases. For an unambiguous gel–fluid (i.e., solid-ordered/liquid-disordered) phase coexistence in binary mixtures of $(14:0)_2$PC and $(16:0)_2$PC, it was found that the presence of gel phase was

associated with the appearance of a fluorescence component of even longer lifetime than that assigned to the L_o phase in cholesterol-containing systems [57]. The binary phase diagram for $(14:0)_2$PC/$(16:0)_2$PC mixtures that was deduced from lifetime analysis of *trans*-parinaric acid and independent determinations of probe partition coefficients is in fair agreement with that deduced from calorimetry (DSC) and the predictions for ideal mixing. Note, however, that the fluorescence lifetime distribution of *trans*-parinaric acid is bimodal in the fluid phase, even in the absence of cholesterol [32,57].

The EPR method that was early introduced for determining L_α–L_o phase boundaries for a range of binary lipid–cholesterol mixtures (Figs. 2B, 3A, 5B, 9B [25]) can only be described as being empirical. Two-component EPR spectra of the spin-labelled lipids, which would be direct evidence for phase coexistence, were not observed. Instead, phase boundaries were determined from discontinuities in gradient of the dependence of the outer hyperfine splittings on cholesterol content for a spin label at the 5-position of the lipid chain. A theoretical model for the dependence was not used, indeed only if the differences in order parameter between coexisting phases were very small would exchange between domains be fast on the EPR timescale (see Eq. (5) and ref. [58]), otherwise an (unresolved) superposition of hyperfine splittings would be obtained.

In several cases, information was obtained solely from differential scanning calorimetry (Figs. 2D [28], 2F [30], 4A [35], 5C [37], 6 [38]). It is a fairly general feature of the excess heat capacity curves of cholesterol-containing lipid mixtures, at least for phosphatidylcholines, that they become broader (and the apparent enthalpy diminishes) at the higher cholesterol contents. This limits the precision with which the phase boundaries, and the existence of a three-phase line, can be established from DSC alone. Particularly it is not easy to define an upper phase boundary with any degree of certainty at high contents of cholesterol. In some cases, the onset of the endotherm remains relatively sharp, with trailing of the tail to higher temperatures [4]. Constancy in temperature of the sharp onset, if found, suggests the existence of a three-phase line, but this is not a feature upon which there is complete agreement.

9. Conclusion

When all these uncertainties are considered together, one is led to the rather disconcerting conclusion that many of the existing phase diagrams for binary mixtures of single lipids with cholesterol may not be quite so solidly based as is generally assumed. Correspondingly, the existence of liquid-ordered phases might also be less ubiquitous than has been anticipated. In so far as lipid rafts may be equated with liquid-ordered phases, conditions for their occurrence are also limited by similar considerations. It appears that ternary mixtures offer more versatile conditions for raft formation than do mixtures of a single lipid with cholesterol.

References

[1] J.H. Ipsen, G. Karlstrom, O.G. Mouritsen, H. Wennerstrom, M.J. Zuckermann, Phase equilibria in the phosphatidylcholine–cholesterol system, Biochim. Biophys. Acta 905 (1987) 162–172.
[2] K. Simons, E. Ikonen, Functional rafts in cell membranes, Nature 387 (1997) 569–572.
[3] K. Simons, W.L. Vaz, Model systems, lipid rafts, and cell membranes, Annu. Rev. Biophys. Biomol. Struct. 33 (2004) 269–295.
[4] M.R. Vist, J.H. Davis, Phase-equilibria of cholesterol dipalmitoylphosphatidylcholine mixtures — ^{2}H nuclear magnetic-resonance and differential scanning calorimetry, Biochemistry 29 (1990) 451–464.
[5] J.L. Thewalt, M. Bloom, Phosphatidylcholine: cholesterol phase diagrams, Biophys. J. 63 (1992) 1176–1181.
[6] A. Blume, R.G. Griffin, Carbon-13 and deuterium nuclear magnetic resonance study of the interaction of cholesterol with phosphatidylethanolamine, Biochemistry 21 (1982) 6230–6242.
[7] S.L. Veatch, S.L. Keller, Seeing spots: complex phase behavior in single membranes, Biochim. Biophys. Acta 1746 (2005) 172–185.
[8] G.W. Feigenson, J.T. Buboltz, Ternary phase diagram of dipalmitoyl-PC/dilauroyl-PC/cholesterol: nanoscopic domain formation driven by cholesterol, Biophys. J. 80 (2001) 2775–2788.
[9] J. Zhao, J. Wu, F.A. Heberle, T.T. Mills, P. Klawitter, G. Huang, G. Constanza, G.W. Feigenson, Phase studies of model biomembranes: complex behavior of DSPC/DOPC/Cholesterol, Biochim. Biophys. Acta 1768 (2007) 2764–2776.
[10] D. Marsh, Cholesterol-induced fluid membrane domains: a compendium of lipid-raft ternary phase diagrams, Biochim. Biophys. Acta 1788 (2009) 2114–2123.
[11] S.L. Veatch, S.L. Keller, Miscibility phase diagrams of giant vesicles containing sphingomyelin, Phys. Rev. Lett. 94 (2005) Art. No. 148101.
[12] J. Zhao, J. Wu, H. Shao, F. Kong, N. Jain, G. Hunt, G.W. Feigenson, Phase studies of model biomembranes: macroscopic coexistence of $L_\alpha + L_\alpha$, with light-induced coexistence of $L_\alpha + L_o$ phases, Biochim. Biophys. Acta 1768 (2007) 2777–2786.
[13] T.T. Mills, S. Tristram-Nagle, F.A. Heberle, N.F. Morales, J. Zhao, J. Wu, G.E.S. Toombes, J.F. Nagle, G.W. Feigenson, Liquid–liquid domains in bilayers detected by wide angle X-ray scattering, Biophys. J. 95 (2008) 682–690.
[14] J.J. Pan, T.T. Mills, S. Tristram-Nagle, J.F. Nagle, Cholesterol perturbs lipid bilayers nonuniversally, Phys. Rev. Lett. 100 (2008) 198103.
[15] M.B. Sankaram, T.E. Thompson, Cholesterol-induced fluid-phase immiscibility in membranes, Proc. Nat. Acad. Sci. USA 88 (1991) 8686–8690.
[16] M.I. Collado, F.M. Goñi, A. Alonso, D. Marsh, Domain formation in sphingomyelin/cholesterol mixed membranes studied by spin-label electron spin resonance spectroscopy, Biochemistry 44 (2005) 4911–4918.
[17] J.H. Davis, J.J. Clair, J. Juhasz, Phase equilibria in DOPC/DPPC-d_{62}/cholesterol mixtures, Biophys. J. 96 (2009) 521–539.
[18] G. Cevc, D. Marsh, Phospholipid bilayers, Physical Principles and Models, Wiley-Interscience, New York, 1987.
[19] P.F.F. Almeida, A. Pokorny, A. Hinderliter, Thermodynamics of membrane domains, Biochim. Biophys. Acta 1720 (2005) 1–13.
[20] T.L. Hill, Thermodynamics of small systems, J. Chem. Phys. 36 (1962) 3182–3197.
[21] J.R. Silvius, Partitioning of membrane molecules between raft and non-raft domains: insights from model-membrane studies, Biochim. Biophys. Acta 1746 (2005) 193–202.
[22] F.M. Goni, A. Alonso, L.A. Bagatolli, R.E. Brown, D. Marsh, M. Prieto, J.L. Thewalt, Phase diagrams of lipid mixtures relevant to the study of membrane rafts, Biochim. Biophys. Acta 1781 (2008) 665–684.
[23] S.L. Veatch, O. Soubias, S.L. Keller, K. Gawrisch, Critical fluctuations in domain-forming lipid mixtures, Proc. Natl. Acad. Sci. USA 104 (2007) 17650–17655.
[24] H.M. McConnell, Understanding membranes, ACS Chem. Biol. 3 (2008) 265–267.
[25] M.B. Sankaram, T.E. Thompson, Interaction of cholesterol with various glycerophospholipids and sphingomyelin, Biochemistry 29 (1990) 10670–10675.
[26] T.-H. Huang, C.W.B. Lee, S.K. Das Gupta, A. Blume, R.G. Griffin, A ^{13}C and ^{2}H nuclear magnetic resonance study of phosphatidylcholine/cholesterol interactions: characterization of liquid-gel phases, Biochemistry 32 (1993) 13277–13287.
[27] A. Blume, R.J. Wittebort, S.K. Das Gupta, R.G. Griffin, Phase equilibria, molecular conformation, and dynamics in phosphatidylcholine/phosphatidylethanolamine bilayers, Biochemistry 21 (1982) 6243–6253.
[28] J.S. Harris, D.E. Epps, S.R. Davio, F.J. Kezdy, Evidence for transbilayer, tail-to-tail cholesterol dimers in dipalmitoylglycerophosphocholine liposomes, Biochemistry 34 (1995) 3851–3857.
[29] T.-X. Xiang, B.D. Anderson, Phase structures of binary lipid bilayers as revealed by permeability of small molecules, Biochim. Biophys. Acta 1370 (1998) 64–76.
[30] R.D. Koynova, A.I. Boyanov, B.G. Tenchov, On the phase diagram of an L-dipalmitoylphosphatidylcholine cholesterol mixture, FEBS Lett. 187 (1985) 65–68.
[31] P.F.F. Almeida, W.L.C. Vaz, T.E. Thompson, Lateral diffusion in the liquid phases of dimyristoylphosphatidylcholine/cholesterol lipid bilayers — a free volume analysis, Biochemistry 31 (1992) 6739–6747.
[32] C. Reyes Mateo, A. Ulises Acuña, J.-C. Brochon, Liquid-crystalline phases of cholesterol/lipid bilayers as revealed by the fluorescence of *trans*-parinaric acid, Biophys. J. 68 (1995) 978–987.
[33] D.J. Recktenwald, H.M. McConnell, Phase equilibria in binary mixtures of phosphatidylcholine and cholesterol, Biochemistry 20 (1981) 4505–4510.
[34] M.J. Ruocco, D.J. Siminovitch, R.G. Griffin, Comparative study of the gel phases of ether-linked and ester-linked phosphatidylcholines, Biochemistry 24 (1985) 2406–2411.
[35] P. Laggner, K. Lohner, R. Koynova, B. Tenchov, The influence of low amounts of cholesterol on the interdigitated gel phase of hydrated dihexadecylphosphatidylcholine, Chem. Phys. Lipids 60 (1991) 153–161.
[36] P.F.F. Almeida, W.L.C. Vaz, T.E. Thompson, Percolation and diffusion in three-component lipid bilayers: effect of cholesterol on an equimolar mixture of two phosphatidylcholines, Biophys. J. 64 (1993) 399–412.
[37] N. Tamai, M. Uemura, T. Takeichi, M. Goto, H. Matsuki, S. Kaneshina, A new interpretation of eutectic behavior for distearoylphosphatidylcholine–cholesterol binary bilayer membrane, Biophys. Chem. 135 (2008) 95–101.
[38] N. Tamai, M. Uemura, M. Goto, H. Matsuki, S. Kaneshina, Lateral phase separation in cholesterol/diheptadecanoylphosphatidylcholine binary bilayer membranes, Colloid Surf. B. : Biointerfaces 65 (2008) 213–219.
[39] Y.W. Chiang, Y. Shimoyama, G.W. Feigenson, J.H. Freed, Dynamic molecular structure of DPPC–DLPC–cholesterol ternary lipid system by spin-label electron spin resonance, Biophys. J. 87 (2004) 2483–2496.
[40] Y.W. Chiang, J. Zhao, J. Wu, Y.H. Shimoyama, J.H. Freed, G.W. Feigenson, New method for determining tie-lines in coexisting membrane phases using spin-label ESR, Biochim. Biophys. Acta 1668 (2005) 99–105.
[41] A. Pokorny, L.E. Yandek, A.I. Elegbede, A. Hinderliter, P.F.F. Almeida, Temperature and composition dependence of the interaction of δ-lysin with ternary mixtures of sphingomyelin/cholesterol/POPC, Biophys. J. 91 (2006) 2184–2197.
[42] G. Lindblom, G. Orädd, Lipid lateral diffusion and membrane heterogeneity, Biochim. Biophys. Acta 1788 (2009) 234–244.
[43] R.M. Epand, R. Bottega, Modulation of the phase transition behavior of phosphatidylethanolamine by cholesterol and oxysterols, Biochemistry 26 (1987) 1820–1825.

[44] D. Bach, E. Wachtel, N. Borochov, G. Senisterra, R.M. Epand, Phase behaviour of heteroacid phosphatidylserines and cholesterol, Chem. Phys. Lipids 63 (1992) 105–113.
[45] F.M. Linseisen, J.L. Thewalt, M. Bloom, T.M. Bayerl, ^{2}H-NMR and DSC study of SEPC–cholesterol mixtures, Chem. Phys. Lipids 65 (1993) 141–149.
[46] J.-H. Sachse, M.D. King, D. Marsh, ESR determination of lipid diffusion coefficients at low spin-label concentrations in biological membranes, using exchange broadening, exchange narrowing, and dipole–dipole interactions, J. Magn. Reson. 71 (1987) 385–404.
[47] A. Filippov, G. Orädd, G. Lindblom, The effect of cholesterol on the lateral diffusion of phospholipids in oriented bilayers, Biophys. J. 84 (2003) 3079–3086.
[48] L.I. Horváth, P.J. Brophy, D. Marsh, Microwave frequency dependence of ESR spectra from spin labels undergoing two-site exchange in myelin proteolipid membranes, J. Magn. Reson. B105 (1994) 120–128.
[49] J.L. Rubenstein, B.A. Smith, H.M. McConnell, Lateral diffusion in binary mixtures of cholesterol and phosphatidylcholine, Proc. Natl. Acad. Sci. USA 76 (1979) 15–18.
[50] A. Filippov, G. Orädd, G. Lindblom, Lipid lateral diffusion in ordered and disordered phases in raft mixtures, Biophys. J. 86 (2004) 891–896.
[51] G. Orädd, P.W. Westerman, G. Lindblom, Lateral diffusion coefficients of separate lipid species in a ternary raft-forming bilayer: a Pfg-NMR multinuclear study, Biophys. J. 89 (2005) 315–320.
[52] G.W. Feigenson, Phase diagrams and lipid domains in multicomponent lipid bilayer mixtures, Biochim. Biophys. Acta 1788 (2009) 47–52.
[53] A. Filippov, G. Orädd, G. Lindblom, Domain formation in model membranes studied by pfg-NMR — the role of lipid polyunsaturation, Biophys. J. 93 (2007) 3182–3190.
[54] H.A. Scheidt, D. Huster, K. Gawrisch, Diffusion of cholesterol and its precursors in lipid membranes studied by 1H pulsed field gradient magic angle spinning NMR, Biophys. J. 89 (2005) 2504–2512.
[55] R.F.M. de Almeida, A. Fedorov, M. Prieto, Sphingomyelin/phosphatidylcholine/cholesterol phase diagram: boundaries and composition of lipid rafts, Biophys. J. 85 (2003) 2406–2416.
[56] R.F.M. de Almeida, L.M.S. Loura, M. Prieto, Membrane lipid domains and rafts: current applications of fluorescence lifetime spectroscopy and imaging, Chem. Phys. Lipids 157 (2009) 61–77.
[57] C.R. Mateo, J.C. Brochon, M.P. Lillo, A.U. Acuna, Lipid clustering in bilayers detected by the fluorescence kinetics and anisotropy of *trans*-parinaric acid, Biophys. J. 65 (1993) 2237–2247.
[58] L.I. Horváth, P.J. Brophy, D. Marsh, Exchange rates at the lipid–protein interface of myelin proteolipid protein studied by spin-label electron spin resonance, Biochemistry 27 (1988) 46–52.
[59] P.L.G. Chong, D. Choate, Calorimetric studies of the effects of cholesterol on the phase transition of C(18):C(10) phosphatidylcholine, Biophys. J. 55 (1989) 551–556.
[60] Y.L. Kao, P.L.G. Chong, C. Huang, Time-resolved fluorometric and differential scanning calorimetric investigation of dehydroergosterol in 1-stearoyl-2-capryl-phosphatidylcholine bilayers, Biochemistry 29 (1990) 1315–1322.
[61] J. Yang, G.L. Anderle, R. Mendelsohn, Effects of cholesterol on the interaction of Ca^{2+}-ATPase with 1-palmitoyl-2-oleoylphosphatidylethanolamine. An FTIR study, Biochim. Biophys. Acta 1021 (1990) 27–32.